Pergamon

PII: S0020-7225(96)00037-7

Int. J. Engng Sci. Vol. 34, No. 12, pp. 1409–1422, 1996

0020-7225/96 $15.00 + 0.00

COMPRESSIBLE TWO-PHASE BOUNDARY-LAYER FLOW WITH FINITE PARTICULATE VOLUME FRACTION

ALI J. CHAMKHA

Department of Mechanical and Industrial Engineering, Kuwait University, P.O. Box 5969, Safat 13060, Kuwait

Abstract—A continuum mathematical model governing compressible boundary-layer fluid-particle flow and heat transfer over a semi-infinite flat plate is developed. This model is based on separate balance laws of mass, linear momentum, and energy for both phases and allows for finite particle-phase volume fraction and viscous stresses. It is found that the volume fraction of suspended particles and, therefore, the particle-phase density is uniform in the boundary layer. Using this fact, the governing nonlinear partial differential equations are simplified and solved numerically by an iterative finite-difference method. Graphical results for flow and heat transfer properties are presented for various values of the particle-fluid viscosity ratio and the power index parameter for the viscosity–temperature relation. Copyright © 1996 Elsevier Science Ltd.

1. INTRODUCTION

Boundary-layer fluid-particle flow has received some attention due to its possible application in various engineering and environmental fields. Some examples are particulate filtration, pollution of city air, flow of blood in arteries, and flow of steam with suspended solid particles over turbine blades. In external boundary-layer flow of a particulate suspension, it is of interest to gain better understanding of physical phenomena such as accumulation of particles near surfaces [1, 2] and the formation of particle-free zone at the walls [3, 4].

The problem of incompressible boundary-layer flow of a dusty fluid over a semi-infinite flat plate has been considered previously by many investigators. Some solved the problem using the series method [5, 6], others used the integral method [7, 8], and others employed finite-difference methods [9, 10]. The compressible version of the same problem has been solved by Singleton [11], and Wang and Glass [12], and Chamkha [13]. Singleton [11] used the series expansion method while Wang and Glass [12], and Chamkha [13] employed the finite-difference technique. In the work by Chamkha [13], general boundary-layer equations for the two-phase suspension are given. These equations include the effect of particulate viscous stresses and general power-law viscosity–temperature relation.

In all the compressible work cited herein, the volume fraction of suspended particles was assumed to be small and the particle phase was assumed pressureless. In the present paper, the volume fraction of particles is assumed to be finite and the particle phase is assumed to behave as a viscous fluid with an analog pressure. All particles are assumed spherical and of one size and the fluid-particle interaction is limited to Stoke's linear drag force and interphase heat transfer.

2. GOVERNING EQUATIONS

Mathematical models of multiphase flow systems have been based on either the Eulerian approach (where both phases are modeled as two interacting continua) or the Lagrangian approach (where only the fluid phase is treated as a continuum and the particle's motion is governed by the kinetic theory). Both approaches are well known from fluid mechanics and

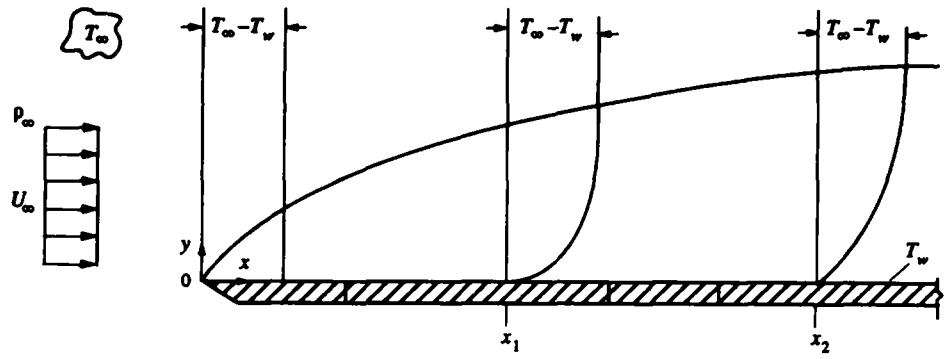

Fig. 1. Flat plate schematic.

are extensively used in the literature [14–16]. In the present work, the Eulerian approach is chosen to represent the motion of the two-phase particulate suspension.

Many investigations of multiphase processes employ continuum models that are restricted to small particulate volume fraction (see [17]). These models assume that the particle phase is dilute in the sense that no particle–particle interaction takes place. While these models may be adequate for some situations where the particle-phase concentration is small, they become inadequate when the particle phase is considered dense. In this case, the continuum dusty-gas models must be modified to account for particle-phase viscous stresses resulting from particle–particle interactions [18].

In some cases, when the original dusty-gas model (which is particle-phase stress-free and restricted to small volume fraction) is employed to model a dense suspension, the predictive results may violate the assumptions inherent in the model. For example, using Marble's [17] model to analyze steady, incompressible, boundary-layer two-phase flow over a semi-infinite plate resulted in a singularity in the particle-phase density at the plate surface (see[6, 19]) which violates the small volume fraction assumption in the model. In this case, a more comprehensive theory is needed to deal with such discontinuities. In the present paper a theory that incorporates the effects of particle-phase viscous stresses and allows for finite particle volume fraction is utilized for modeling of compressible dusty-gas boundary-layer flow over a semi-infinite flat plate.

Consider steady, compressible, laminar, boundary-layer flow of a two-phase suspension along a semi-infinite flat plate with a free-stream velocity U_∞ and a free-stream temperature T_∞. Let the surface temperature be T_w, which is constant (see Fig. 1). No slip condition at the plate surface requires that the fluid velocity vanishes there. Thus, the velocity of the fluid will vary within a small region close to the wall from 0 to U_∞, and the fluid temperature will vary from $T_w$to T_∞. This causes the development of the hydrodynamic and thermal boundary layers for this type of flow. In addition, momentum and heat exchanges occur between the fluid and the particles suspended in it. In this work, the fluid is assumed to behave as a perfect gas, and the particle phase is assumed to have a pressure.

To model such a flow situation by the continuum approach, the balance laws of mass, linear momentum, and energy of both phases must be considered. These can be written, respectively, as

$$\vec{\nabla}.(\rho\vec{V}) = 0,\ \vec{\nabla}.(\rho_p\vec{V}_p) = 0$$

$$\rho\vec{V}.\vec{\nabla}\vec{V} = \vec{\nabla}.\underline{\underline{\sigma}} - \vec{S}_\ell,\ \rho_p\vec{V}_p.\vec{\nabla}\vec{V}_p = \vec{\nabla}.\underline{\underline{\sigma}}_p + \vec{S}_\ell$$

$$\rho c\vec{V}.\vec{\nabla}T = \vec{\nabla}.(k\vec{\nabla}T) + \underline{\underline{\sigma}}:\vec{\nabla}\vec{V} + (\vec{V} - \vec{V}_p).\vec{S}_\ell + Q_T$$

$$\rho_p c_p\vec{V}_p.\vec{\nabla}T_p = \underline{\underline{\sigma}}_p:\vec{\nabla}\vec{V}_p - Q_T \tag{2.1}$$

where ρ, $\vec{V}$, $\underline{\underline{\sigma}}$, c, k, and T are the fluid-phase density, velocity vector, stress tensor, specific

heat, thermal conductivity, and temperature, respectively. Properties and variables with subscript p denote the same thing for the particle phase. Also, $\vec{\nabla}$ is the gradient operator and $\vec{S}_\ell$ and Q_T are the interphase force per unit volume of suspension, and the interphase heat transfer, respectively.

Equations (2.1) are supplemented by the following constitutive equations:

$$\underline{\underline{\sigma}} = -P\underline{\underline{I}} + \mu(T)(\vec{\nabla}\vec{V} + \vec{\nabla}\vec{V}^{\mathrm{T}})$$

$$\underline{\underline{\sigma}}_{\mathrm{p}} = -P_{\mathrm{p}}\underline{\underline{I}} + \mu_{\mathrm{p}}(T)(\vec{\nabla}\vec{V}_{\mathrm{p}} + \vec{\nabla}\vec{V}_{\mathrm{p}}^{\mathrm{T}})$$

$$\vec{S}_\ell = \rho_{\mathrm{p}} N(\vec{V} - \vec{V}_{\mathrm{p}}),\quad Q_T = \rho_{\mathrm{p}} c_{\mathrm{p}} N_T (T_{\mathrm{p}} - T)$$

$$P = \rho RT,\ P_{\mathrm{p}} = DN\rho_{\mathrm{p}} \tag{2.2}$$

where P is the fluid-phase pressure, $\underline{\underline{I}}$ is the unit tensor, μ and μ_{p} are fluid and particle-phase viscosity coefficients, respectively, N and N_T are the momentum and heat transfer coefficients, respectively, R is the gas constant, D is the interphase diffusion coefficient, and a superposed T denotes the transpose of a second-order tensor, respectively.

Substituting equations (2.2) into equations (2.1) and performing a standard boundary-layer order-of-magnitude analysis similar to that discussed in detail by Chamkha and Peddieson [20, 21] shows that the particle-phase density in the boundary layer is uniform and is equal to the free stream value. This prediction was used previously by Chiu [22] in his analysis of boundary layer flow with suspended particles.

Using this fact and substituting the modified Blasius transformations

$$x = U_\infty \xi/(N(1-\xi)),\ y = U_\infty/(N\,\mathrm{Re}_\infty^{1/2})(2\xi/(1-\xi))^{1/2}\eta$$

$$\vec{V} = U_\infty(F(\xi,\eta)\vec{e}_x + ((1-\xi)/(2\xi))^{1/2}(G(\xi,\eta) + \eta F(\xi,\eta))/\mathrm{Re}_\infty^{1/2}\vec{e}_y)$$

$$\vec{V}_{\mathrm{p}} = U_\infty(F_{\mathrm{p}}(\xi,\eta)\vec{e}_x + ((1-\xi)/(2\xi))^{1/2}(G_p(\xi,\eta) + \eta F_{\mathrm{p}}(\xi,\eta))/\mathrm{Re}_\infty^{1/2}\vec{e}_y)$$

$$T = T_\infty H(\xi,\eta),\ T_{\mathrm{p}} = T_\infty H_{\mathrm{p}}(\xi,\eta),\ \rho = \rho_\infty Q(\xi,\eta),\ \rho_{\mathrm{p}} = \rho_{\mathrm{p}\infty}$$

$$\mu = \mu_\infty H(\xi,\eta)^\omega,\ \mu_{\mathrm{p}} = \mu_{\mathrm{p}\infty} H_{\mathrm{p}}(\xi,\eta)^\omega$$

$$\mathrm{Pr} = \mu c/k,\ \mathrm{Ec} = U_\infty^2/(cT_\infty)$$

$$\beta = \mu_{\mathrm{p}\infty}/\mu_\infty,\ \gamma = c/c_{\mathrm{p}} \tag{2.3}$$

(where ξ and η are transformed tangential and normal distances, respectively; F, G, H, and Q are transformed fluid-phase tangential velocity, normal velocity, temperature, and density, respectively; F_{p}, G_{p}, and H_{p} are transformed particle-phase tangential velocity, normal velocity, and temperature, respectively; Pr, Ec, β, and γ are the Pandtl number, Eckert number, free stream viscosity ratio, and ratio of specific heats, respectively; $\mathrm{Re}_\infty = \rho_\infty U_\infty^2/(N\mu_\infty)$, e denotes a unit vector, and U_∞, ρ_∞, μ_∞ and T_∞ are the fluid free-stream velocity, density, dynamic viscosity, and temperature, respectively; $\rho_{\mathrm{p}\infty}$ ($=\rho_\infty$) and $\mu_{\mathrm{p}\infty}$ are particle-phase free-stream density and dynamic viscosity, respectively; and ω is a power index, a constant such that $0.5 \le \omega \le 1$) into the resulting boundary-layer equations yield

$$\partial_\eta(QG) + QF + 2\xi(1-\xi)\partial_\xi(QF) = 0 \tag{2.4}$$

$$H^\omega \partial_\eta^2 F + (\omega H^{\omega-1}\partial_\eta H - QG)\partial_\eta F - 2\xi/(1-\xi)((1-\xi)^2 QF\partial_\xi F - H^\omega(F_p - F)) = 0 \tag{2.5}$$

$$\beta H^\omega{}_{\mathrm{p}}\partial_\eta F_{\mathrm{p}} + (\beta\omega H_{\mathrm{p}}^{\omega-1}\partial_\eta H_{\mathrm{p}} - G_{\mathrm{p}})\partial_\eta F_{\mathrm{p}} - 2\xi/(1-\xi)[(1-\xi)^2 F_{\mathrm{p}}\partial_\xi F_{\mathrm{p}} + H^\omega(F_{\mathrm{p}} - F)] = 0 \tag{2.6}$$

$$\beta H_{\mathrm{p}}^\omega \partial_\eta^2 G_{\mathrm{p}} + (\beta\omega H_{\mathrm{p}}^{\omega-1}\partial_\eta H_{\mathrm{p}} - G_{\mathrm{p}})\partial_\eta G_{\mathrm{p}} - \beta H_{\mathrm{p}}^\omega \partial_\eta^2(\eta F_{\mathrm{p}}) + \beta\omega H_{\mathrm{p}}^{\omega-1}\partial_\eta H_{\mathrm{p}}\partial_\eta(\eta F_{\mathrm{p}}) - \eta G_{\mathrm{p}}\partial_\eta F_{\mathrm{p}}$$
$$+ \eta F_{\mathrm{p}}^2 - 2\xi(1-\xi)F_{\mathrm{p}}\partial_\xi(G_{\mathrm{p}} + \eta F_{\mathrm{p}}) - 2\xi/(1-\xi)H^\omega(G_{\mathrm{p}} - G + \eta(F_{\mathrm{p}} - F)) = 0 \tag{2.7}$$

$$H^\omega \partial_\eta^2 H + (\omega H^{\omega-1}\partial_\eta H - \mathrm{Pr}\,QG)\partial_\eta H - 2\xi(1-\xi)\mathrm{Pr}\,QF\partial_\xi H + \mathrm{EcPr}H^\omega(\partial_\eta F)^2$$
$$+ 2\xi/(1-\xi)(\mathrm{EcPr}H^\omega(F_{\mathrm{p}} - F)^2 + 2H^\omega(H_{\mathrm{p}} - H)/3) = 0 \tag{2.8}$$

$$G_p\partial_\eta H_p - \beta \mathrm{Ec}\gamma H_p^{\omega}(\partial_\eta F_p)^2 + 2\xi(1-\xi)F_p\partial_\xi H_p + 4\xi/(1-\xi)\gamma H^{\omega}(H_p - H)/(3\mathrm{Pr}) = 0 \quad (2.9)$$

$$QH = 1. \quad (2.10)$$

The physics of the problem suggests the following boundary conditions:

$$F(\xi,0) = 0,\ F(\xi,\infty) = 1,\ G(\xi,0) = 0$$

$$H(\xi,0) = h_0,\ H(\xi,\infty) = 1,\ F_p(\xi,0) = S((1-\xi)/(2\xi))^{1/2}\partial_\eta F_p(\xi,0)$$

$$F_p(\xi,\infty) = 1,\ G_p(\xi,0) = 0$$

$$G_p(\xi,\infty) = G(\xi,\infty),\ H_p(\xi,\infty) = 1,\ Q(\xi,\infty) = 1 \quad (2.11)$$

where $h_0 = T_w/T_\infty$ and S are constants.

It should be mentioned that the use of the modified Blasius transformations allows the governing equations of the present problem to be solved analytically at the leading edge of the plate. It can be seen that when ξ is set equal to zero in equations (2.6), (2.7) and (2.9), then these equations are identically satisfied by the solutions $F_p = 1$, $G_p = -\eta$, and $H_p = 1$, respectively. Solution of the fluid-phase equations at $\xi = 0$ is governed by the Blasius solution of incompressible flow past a semi-infinite flat plate. In contrast, Wang and Glass [12] employ solutions produced by the asymptotic expansion method as the initial profiles of flow properties to start the finite-difference procedure and to avoid the singularities associated with the leading edge of the plate. Another advantage of the modified Blasius transformations is that they convert the computational domain from semi-infinite in x $(0 \le x < \infty)$ to finite in ξ $(0 \le \xi \le 1)$.

The first and third equations of the boundary conditions given in (2.11) indicate that the fluid phase does not slip at the wall in the tangential and normal directions, respectively. The sixth equation of (2.11) indicates that the particle phase can experience wall slip ($S \neq 0$). This type of boundary condition is similar to that used in rarefied gas dynamics. It is employed herein since the exact form of boundary conditions for a particle phase at a surface is not known at present, and because a system of particles may resemble a rarefied gas. The fourth and eighth equations of (2.11) indicate that the fluid phase has no temperature jump at the wall, and the particle phase has a no slip condition in the normal direction at the wall, respectively. The remaining equations of (2.11) indicate that far above the plate all variables are in equilibrium with the free-stream conditions. It should be noted that it is an experimental fact that in a laminar boundary-layer flow of a particulate suspension there is a very thin region in the immediate vicinity of the surface occupied by the fluid phase only. Thus, the particle phase is not in direct contact with the wall and is separated from it by that thin region of the fluid. Therefore, it is reasonable to assume that the particle phase slips at the wall while the fluid phase does not.

In external boundary-layer flows, the development of the boundary layer, the wall flow resistance, and the wall heat transfer along the surface of the body are of special importance. This is due to their use in optimizing the design of the body. For the two-phase particulate suspension situation considered herein, the displacement thicknesses, the skin-friction coefficients for both the fluid and the particle phases, and the wall heat transfer coefficient can be defined, respectively, as

$$\Delta(\xi) = \int_0^\infty (1 - QF)\mathrm{d}\eta,\ \Delta_p(\xi) = \int_0^\infty (1 - F_p)\mathrm{d}\eta$$

$$C(\xi) = H(\xi,0)^{\omega}\partial_\eta F(\xi,0),\ C_p(\xi) = \beta H_p(\xi,0)^{\omega}\partial_\eta F_p(\xi,0)$$

$$q_w(\xi) = H(\xi,0)^{\omega}\partial_\eta H(\xi,0)/(\mathrm{EcPr}) \quad (2.12)$$

It should be noted that the definition of C_p is put in terms of β to represent additional shear effects of particles.

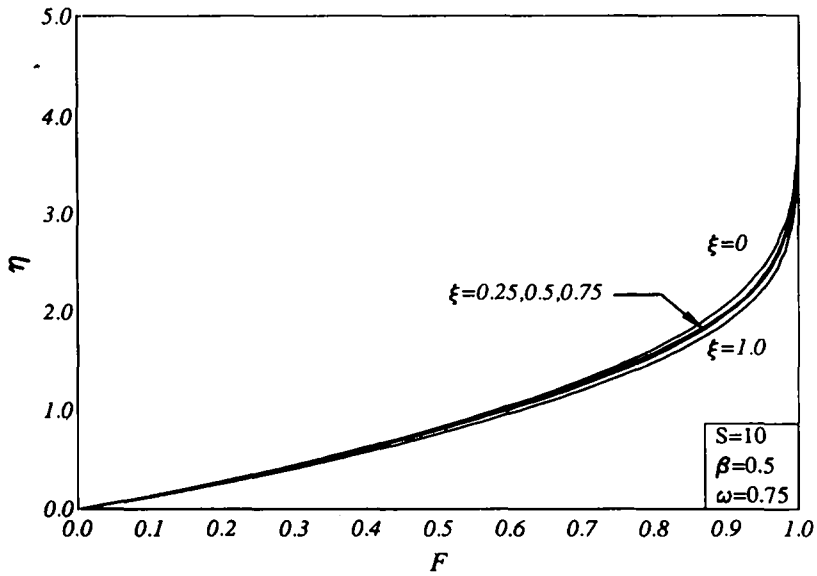

Fig. 2. Fluid-phase tangential velocity profiles.

3. RESULTS AND DISCUSSION

Contrary to the case of single-phase flow, no similarity solutions exist for the present problem. As is obvious from equations (2.4)–(2.10), the nature of these equations is highly nonlinear and, therefore, must be solved numerically. The tri-diagonal, implicit, finite-difference scheme discussed by Blottner [23] has proved to be successful for the solution of such equations. It is, therefore, selected for the numerical solution of the problem under consideration.

The problem was solved as an initial-value problem with ξ playing the role of time. A 1000×196 grid (in ξ and η, respectively) is utilized. Constant step sizes in ξ ($\Delta\xi = 0.001$) and variable step sizes in η (with the smallest step size ($\Delta\eta_1 = 0.001$) adjacent to the plate surface where significant variations from uniformity are expected) were employed. A growth factor of 1.03 was used in the η direction. It should be mentioned that the step sizes used in the present

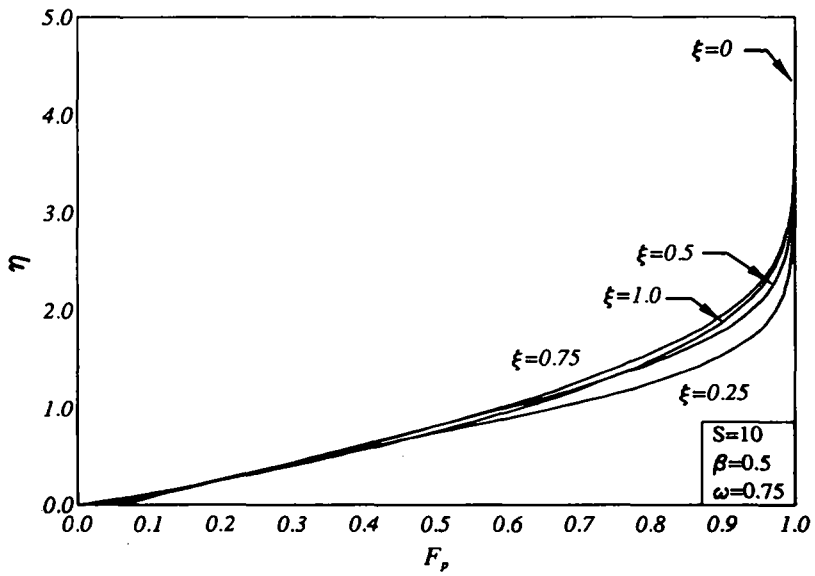

Fig. 3. Particle-phase tangential velocity profiles.

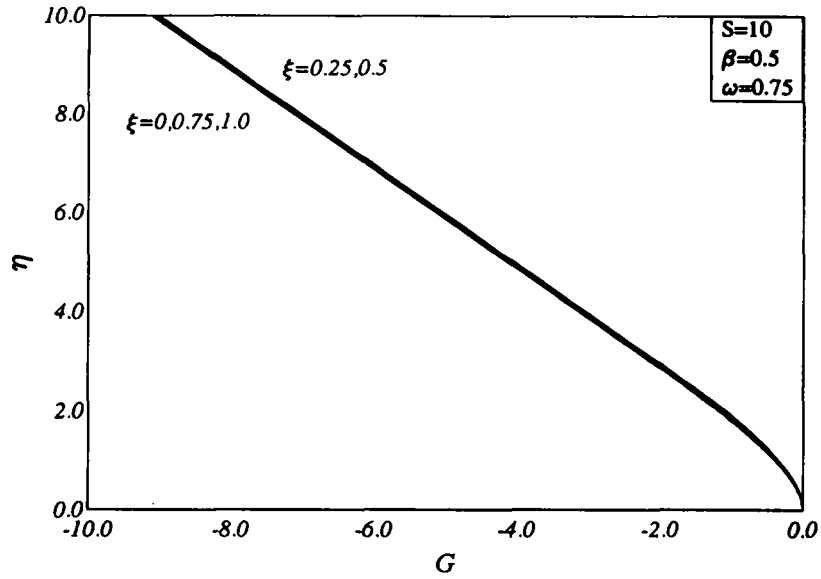

Fig. 4. Fluid-phase normal velocity profiles.

work were chosen as a result of many numerical tests (by reducing the step sizes in both directions) which were performed to ensure grid independence. All derivatives with respect to ξ were represented by two-point backward difference quotients. Derivatives with respect to η in the second-order equations in η were represented by three-point central difference quotients while η differencing in the first-order equations in η was accomplished by the trapezoidal rule. The solution was obtained line by line starting at $\xi = 0$ and marching downstream toward $\xi = 1$. As mentioned before using equation (2.3), exact equations were solved at $\xi = 0$ instead of assuming initial profiles for the flow variables as was usually done when working with the original untransformed variables. Because the governing equations are nonlinear, iteration was used at each line of constant ξ. As a result, a tri-diagonal matrix of linear algebraic equations was created and was solved numerically by the Thomas' algorithm as discussed by Blottner [23]. The iteration process was continued until convergence of the desired solution occurred

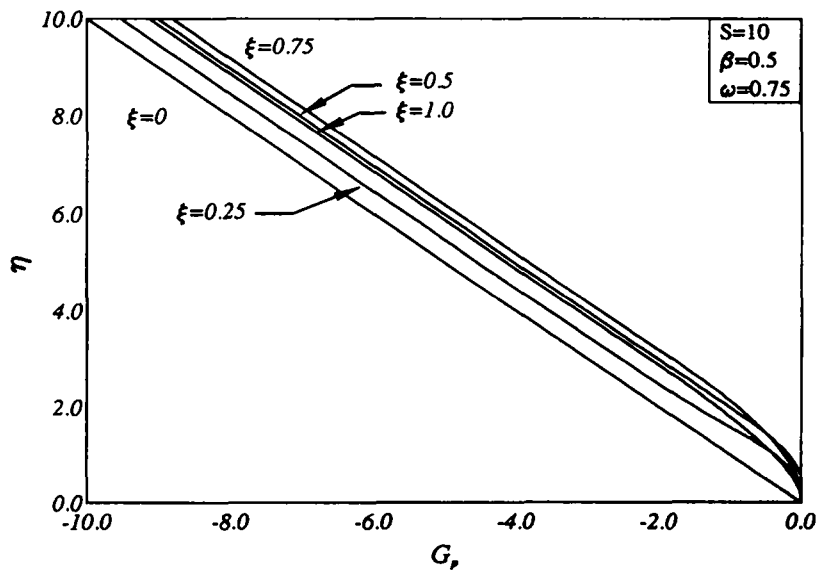

Fig. 5. Particle-phase normal velocity profiles.

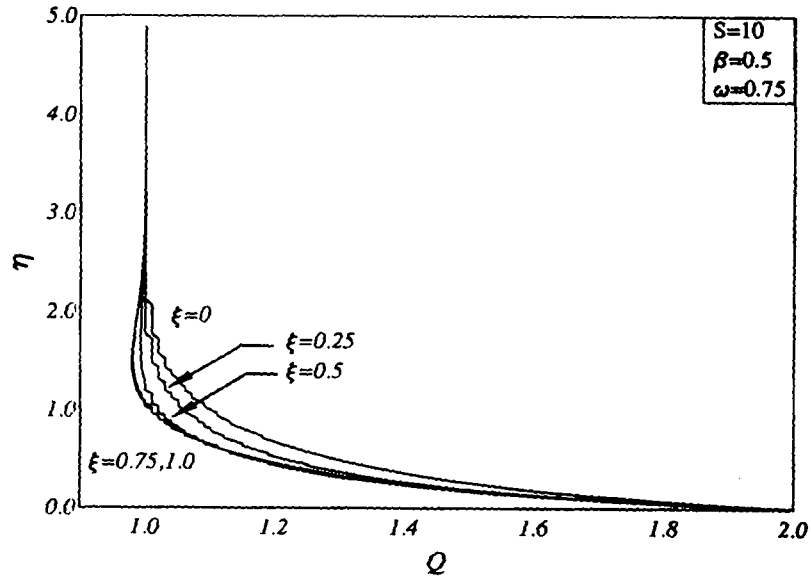

Fig. 6. Fluid-phase density profiles.

within certain acceptable limits (when the difference between the current and the previous iterations was 10^{-5} in this case).

Figures 2–5 illustrate the development of the velocity profiles in the tangential and transformed normal directions of both the fluid and particle phases. A fast transition from frozen flow (where both phases move independently) at $\xi = 0$ to equilibrium flow (where both phases move together) at $\xi = 1$ is observed especially for the fluid's tangential and normal velocity components. For the parametric values used to obtain these results, it is seen that the particle phase is allowed to experience a small amount of slip. The amount of slip is controlled by the slip coefficient S.

Figures 6–8 present typical profiles for the fluid-phase density and temperature, and the particle-phase temperature, respectively. Equation (2.10) implies that the fluid-phase density varies as the reciprocal of its temperature. Since the wall temperature h_0 is taken to be 0.5, then Q at the wall must be 2.0 and Q is decreased as η is increased until it reaches unity

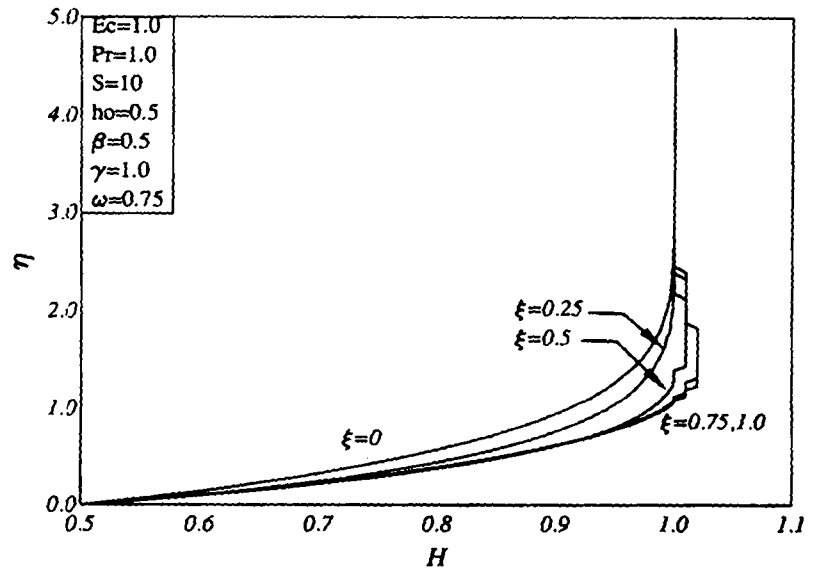

Fig. 7. Fluid-phase temperature profiles.

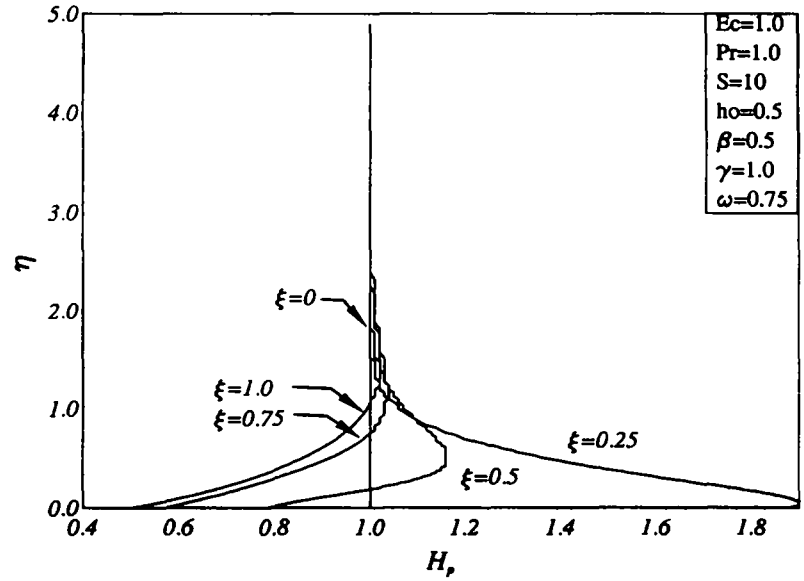

Fig. 8. Particle-phase temperature profiles.

(the free-stream value). This smooth approach of Q to the free-stream conditions is depicted in Fig. 6.

The effects due to the presence of the particle-phase viscosity on the flow and heat transfer properties are shown in Figs 9–13. These figures present representative profiles for the fluid-phase displacement thickness Δ, the particle-phase displacement thickness Δ_p, the fluid-phase skin-friction coefficient C, the particle-phase skin-friction coefficient C_p, and the wall heat transfer coefficient q_w, respectively. Physically speaking, at the leading edge of the plate, the slip velocity and, therefore, the drag force between the two phases is maximum. This momentum transfer mechanism between the phases decreases as the flow moves downstream. During this momentum exchange, the particle-phase tangential velocity increases as it tries to become equal with that of the fluid phase except in the immediate vicinity of the wall. This causes the displacement thickness of the particle phase to increase as ξ increases as illustrated in Fig. 10. Although the fluid tangential velocity decreases due to the presence of particles, the

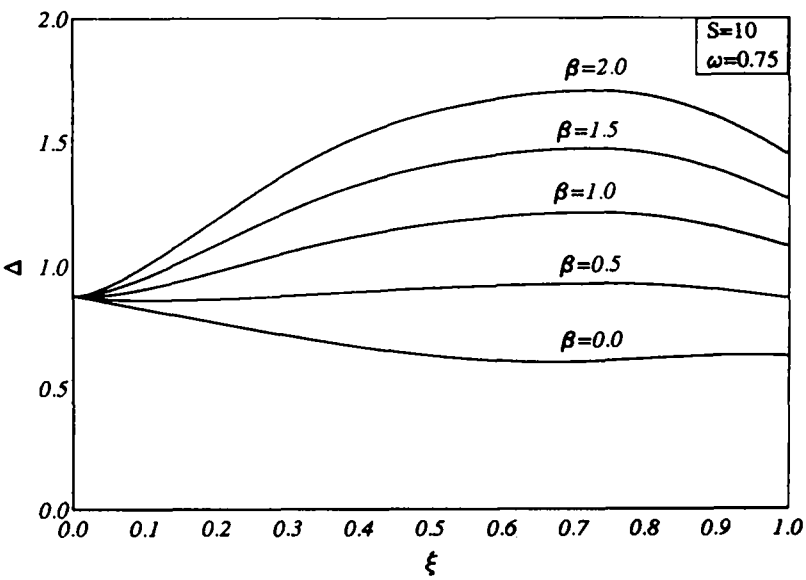

Fig. 9. Fluid-phase displacement thickness profiles.

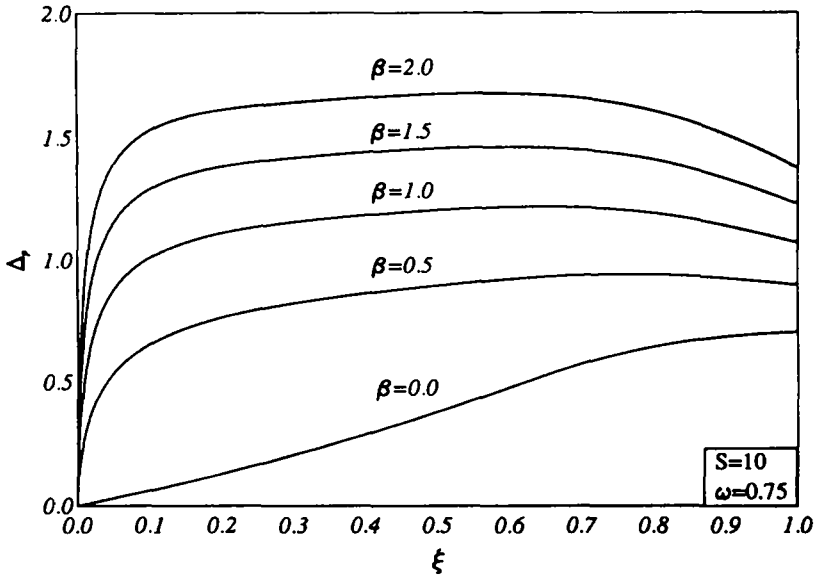

Fig. 10. Particle-phase displacement thickness profiles.

fluid-phase displacement thickness seems to increase over most of the computational domain (except for $\beta = 0$) and then decreases close to $\xi = 1$. This increase in Δ is due to the fluid density variation along the plate (see the definition of Δ). An increase in the displacement thickness causes the slope of the tangential velocity at the wall to decrease. This causes the skin friction coefficient to decrease. This can be said for both the fluid and particle phases. These behaviors are illustrated in Figs 11 and 12.

Increasing the viscosity ratio β has the tendency to increase the effective viscosity of the suspension. This causes both Δ and Δ_p to increase more rapidly. This follows a rapid decrease in the values of C due to the inverse relation between Δ and C mentioned before. The values of C_p also increase as β increases since C_p is defined as directly proportional to β. These behaviors are clearly evident from Figs 9–12. The behavior of the wall heat transfer coefficient q_w is generally similar to that of C along the plate. However, q_w seems to increase as β increases

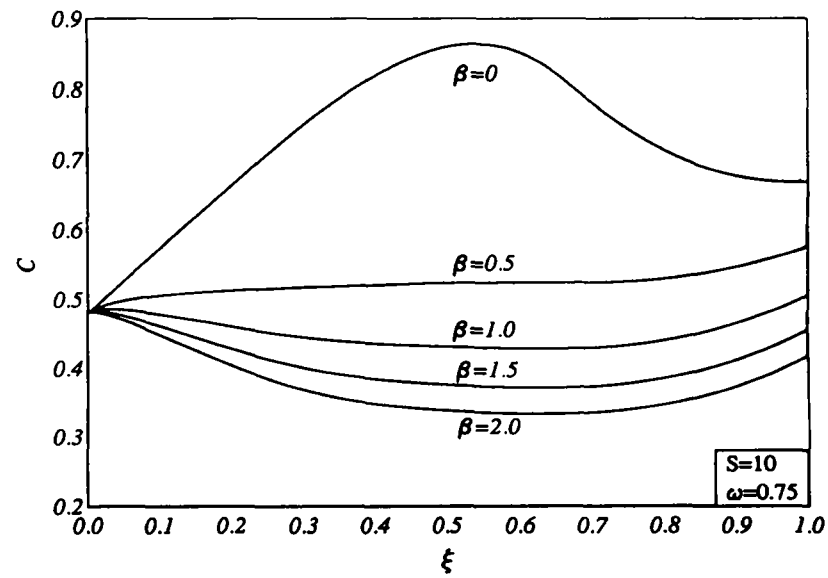

Fig. 11. Fluid-phase skin friction coefficient profiles.

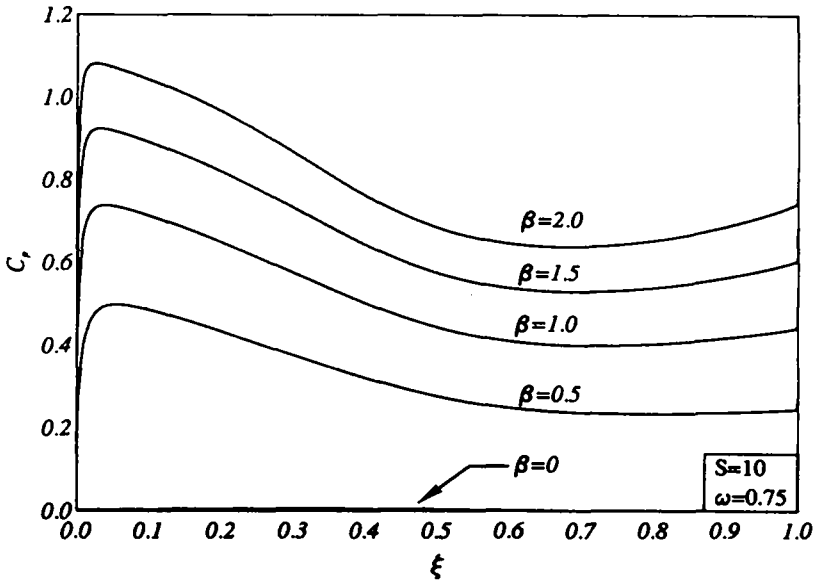

Fig. 12. Particle-phase skin friction coefficient profiles.

(except for $\beta = 0$ which has the highest value). This is probably due to the increase in the work energy which results from higher values of β.

Figures 14–18 are obtained by fixing the values of β and S and allowing the power index ω to vary. These figures illustrate the influence of ω on the flow and heat transfer properties. Figures 14 and 15 present the development of the fluid- and particle-phase displacement thicknesses along the plate for various values of ω, respectively. It is seen from these figures that increasing ω causes Δ and Δ_p to decrease and increase slightly especially close to the plate's leading edge.

Figures 16 and 17 show profiles for the fluid- and particle-phase skin-friction coefficients along the plate for different values of ω, respectively. It can be shown from the definitions of C and C_p [equations (2.12)] that they are directly proportional to the wall viscosities of the fluid and particle phases, respectively. These viscosities are dependent on the wall temperatures which are constant for the fluid phase ($h_0 = 0.5$) and variable for the particle phase. Thus,

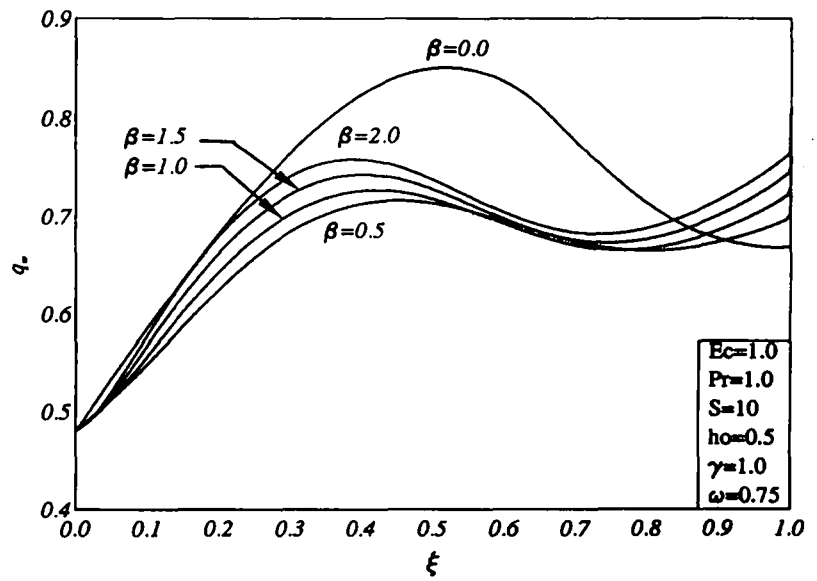

Fig. 13. Wall heat transfer coefficient profiles.

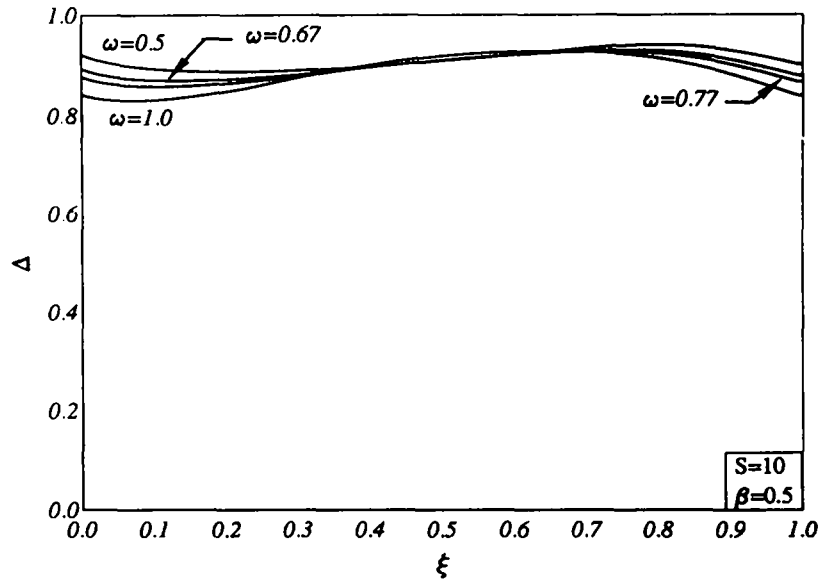

Fig. 14. Fluid-phase displacement thickness profiles.

increasing ω causes $H(\xi,0)^{\omega}$ and $H_p(\xi,0)^{\omega}$ to decrease and increase, respectively. Therefore, the direct effect of increasing ω is a decrease in C and an increase in C_p as depicted in Figs 16 and 17, respectively.

Figure 18 presents the variations in the wall heat transfer coefficient q_w along the tangential distance ξ as a result of changing ω. Physically, as ω increases the fluid-phase wall viscosity and thermal conductivity decrease for the reasons mentioned above. This yields a decrease in the values of q_w at any position along the plate as shown in Fig. 18.

The equations for incompressible two-phase flow with constant finite volume fraction reported previously by Chamkha and Peddieson [20] can be recovered from the equations presented in this paper by making the appropriate assumptions. Therefore, when the finite-difference equations of the present work were modified for the incompressible case, excellent agreement with the solutions given in [20] were achieved. This helped to verify the correctness of the numerical results reported in this paper. It should be mentioned that the

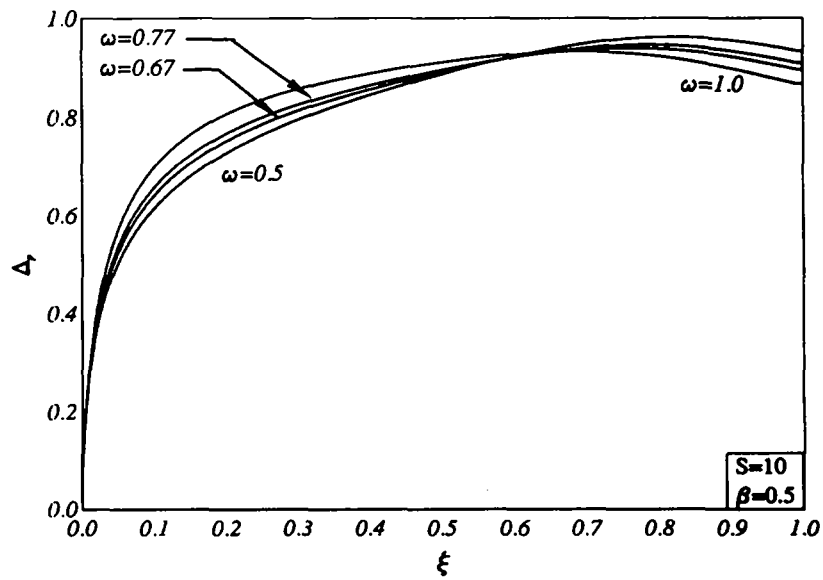

Fig. 15. Particle-phase displacement thickness profiles.

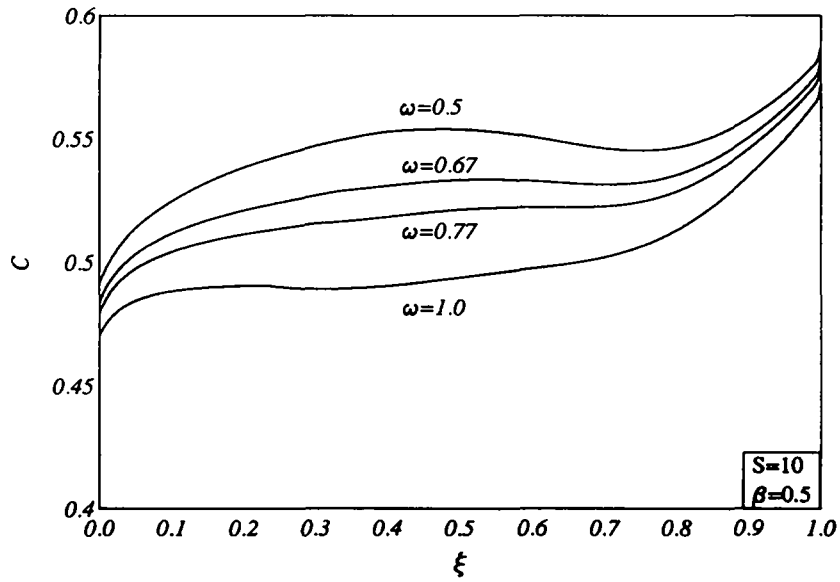

Fig. 16. Fluid-phase skin friction coefficient profiles.

results presented herein, however, are in marked contrast with the work of Chamkha and Peddieson [21] since the particle-phase wall density vanishes therein. The validity of the different models can be best accomplished by comparison with experimental data. As far as the author is aware, such data are lacking at present. For this reason, it is difficult to determine which model is physically accurate. In addition, no direct comparisons with the works of Singleton [11] and Wang and Glass [12] are possible since their results are applicable for particle-phase stress-free and variable particle-phase density.

4. CONCLUSION

In the present paper the boundary-layer equations for steady, laminar, compressible flow past a semi-infinite flat plate were developed using a typical model describing a fluid-particle suspension having a finite volume fraction. An obvious boundary layer order of magnitude

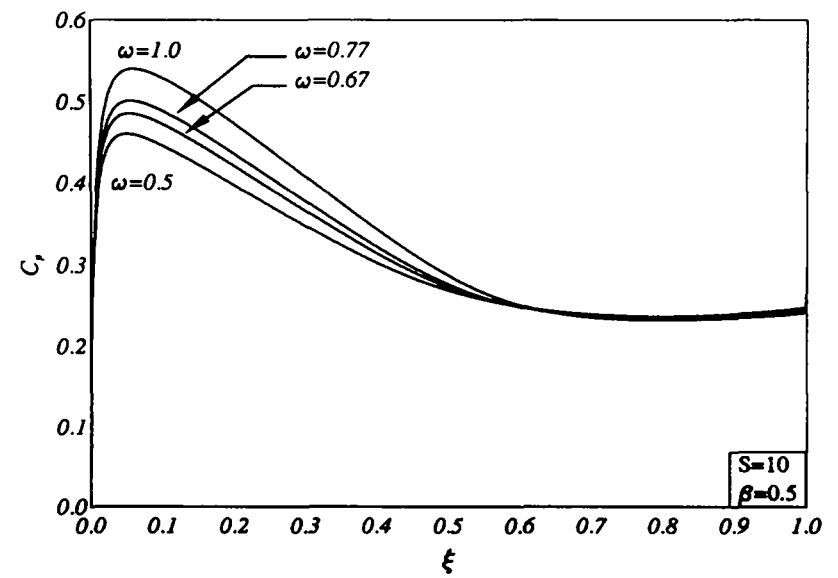

Fig. 17. Particle-phase skin friction coefficient profiles.

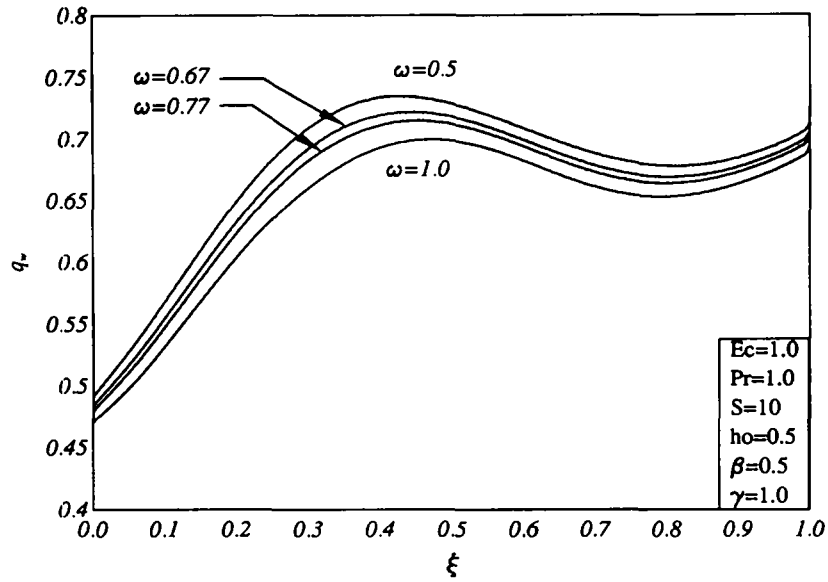

Fig. 18. Wall heat transfer coefficient profiles.

analysis showed that the volume fraction (and, consequently, the density) of the particle-phase was constant in the boundary layer. This result is in marked contrast to the work of previous investigators who employed the original dusty-gas model which is restricted to small volume fractions. The work reported herein illustrates the significance of model selection in two-phase flow analysis.

Some representative numerical results were shown graphically to illustrate the influence of the particle-phase viscosity and the power index for the viscosity–temperature relation on the flow and heat transfer properties. It was found that increases in the viscosity ratio β caused increases in the displacement thicknesses of both phases Δ and Δ_p as well as the particle-phase skin-friction coefficient C_p and decreases in the fluid-phase skin-friction coefficient C and wall heat transfer coefficient q_w. Also, increases in the viscosity–temperature power index coefficient ω resulted in decreases in Δ, C and q_w and increases in Δ_p and C_p. Because of the simplicity introduced by a constant particle-phase volume fraction, it is felt that the present model would be a useful vehicle for the investigation of alternate particle-phase stress models and particle-phase boundary conditions.

Acknowledgement—The author wishes to acknowledge and thank the Research Administration of Kuwait University for funding this project under grant number EPM-079. Also, special thanks are due to Khalil Khanafer for producing the graphs used in this paper.

REFERENCES

[1] A.J. CHAMKHA and J. PEDDIESON, *Proc. of the Thirteenth Canadian Congress of Applied Mechanics* **2**, 474 (1991).
[2] G.F. CARRIER, *J. Fluid Mech.* **4**, 376 (1958).
[3] A.J. CHAMKHA and J. PEDDIESON, *Computational Methods and Experimental Measurements V*. Elsevier Applied Science, London, New York (1991).
[4] A. KARMIS *et al.*, *Canadian J. Chemical Engng* **18**, 181 (1966).
[5] S.L. SOO, *ZAMP*, **19**, 545 (1968).
[6] N. DATTA and S. K. MISHRA, *Acta Mechanica* **42**, 71 (1982).
[7] S.L. SOO, *Fluid Dynamics of Multiphase Systems*. Blaisdell Publishing Co., Waltham, MA (1967).

[8] S.L. SOO, University of Illinois, Project Squid Report ILL-3P (1961).
[9] A.J. CHAMKHA and J. PEDDIESON, *Developments in Mechanics* **15,** 315 (1989).
[10] S. PRABHA and A.C. JAIN, *Appl. Sci. Res.* **36** 81 (1980).
[11] R.E. SINGLETON, *ZAMP* **16,** 421 (1965).
[12] B.Y. WANG and I.I. GLASS, *J. Fluid Mech.* **186,** 223 (1988).
[13] A.J. CHAMKHA, *ASME J. Fluids Engng* (in press).
[14] S.L. SOO, *Particulates and Continuum: Multiphase Fluid Dynamics*. Hemisphere Publishing Corporation, New York (1989).
[15] M. ISHII, *Thermo-Fluid Dynamics Theory of Two-Phase Flow*. Eyrolles, Paris (1975).
[16] A. BERLEMONT, G. GRANCHER and A. GOUESBET, *Int. J. Mass and Heat Transfer* **34,** 2805 (1991).
[17] F.E. MARBLE, *Annual Rev. Fluid Mech.* **2,** 397 (1970).
[18] M. GADIRAJU, J. PEDDIESON and S. MUNUKUTLA, *Mech. Res. Comm.* **19,** 7 (1992).
[19] A.N. OSIPTSOV, *Fluid Dynamics* **15,** 512 (1980).
[20] A.J. CHAMKHA and J. PEDDIESON, *Engng Sci. Preprints* **27,** 1 (1990).
[21] A.J. CHAMKHA and J. PEDDIESON, *ASME J. Fluids Engng* **116,** 147 (1994).
[22] H.H. CHIU, Report 620, Princeton University (1962).
[23] F.G. BLOTTNER, *AIAA J.* **8,** 193 (1970).

(Received 30 December 1994; accepted 29 January 1996)